Photothermal Reactions Hot Paper

International Edition: DOI: 10.1002/anie.201412103
German Edition: DOI: 10.1002/ange.201412103

Graphene Liquid Marbles as Photothermal Miniature Reactors for Reaction Kinetics Modulation**

Wei Gao, Hiang Kwee Lee, Jonathan Hobley, Tianxi Liu, In Yee Phang,* and Xing Yi Ling**

Abstract: *We demonstrate the fabrication of graphene liquid marbles as photothermal miniature reactors with precise temperature control for reaction kinetics modulation. Graphene liquid marbles show rapid and highly reproducible photothermal behavior while maintaining their excellent mechanical robustness. By tuning the applied laser power, swift regulation of graphene liquid marble's surface temperature between 21–135 °C and its encapsulated water temperature between 21–74 °C are demonstrated. The temperature regulation modulates the reaction kinetics in our graphene liquid marble, achieving a 12-fold superior reaction rate constant for methylene blue degradation than at room temperature.*

Liquid marbles are formed by the spontaneous encapsulation of liquid droplets by pulverized solid particles.[1] They are promising miniature reactors owing to their ability to isolate microliter liquid, ease of fabrication, and excellent mechanical robustness.[2] Such miniature reactor is ideal for reactions involving costly and hazardous reagents/processes, and useful in preliminary reaction screening. Liquid marble reactors have been applied for blood typing,[3] nanocomposite synthesis,[4] photochemical polymerization,[5] and heterogeneous catalysis.[6] However, current applications of liquid marble reactors are restricted to reactions of low activation energy or at room temperature due to the lack of a heating mechanism. It is essential to incorporate a heating mechanism into liquid marble to broaden its application for reactions requiring precise control and elevated temperature.

Graphene is a promising candidate for heatable liquid marble miniature reactor due to their excellent photothermal properties.[7] Their strong photoabsorption over a wide range of wavelengths allows rapid and localized heating upon vibrational relaxation of photoexcited electrons.[8] Currently, the incorporation of graphene are mainly in the form of suspensions or films,[9] which require tedious reactant/product recovery procedures, and/or film fabrication protocols. Hence, the combination of graphene and liquid marble allows easy-to-prepare heatable miniature reactor, and permits a broad range of processes with precise temperature and reaction kinetic control. Notably, the localized photothermal heating is crucial as thermal energy is supplied to the small-volume reaction on-demand without changing the bulk liquid medium temperature.[10] This reduces the evaporation issues of miniature reactors and minimizes energy waste, making it superior to conduction/convection heating.[10]

Herein, we demonstrate the fabrication of graphene liquid marbles (GLM) and their application as remotely heatable miniature reactors for reaction kinetic modulation. The physical and mechanical properties of GLM as isolated and robust miniature reactors are characterized. We then demonstrate the instant heating of GLM with surface temperatures tunable between 21 to 135 °C by controlling the laser power. The actual encapsulated water temperature is probed using temperature-dependent Raman scattering spectroscopy. The application of GLM for reaction kinetics modulation is subsequently evaluated by performing a temperature-dependent degradation of methylene blue. We also highlight the easy post-reaction recovery of encapsulated liquid and emphasize the superior photothermal properties of GLM over other materials.

GLM are fabricated by rolling microliter water droplets on a bed of pulverized perfluorooctylysilane-grafted graphene nanoplatelets (thickness $\approx$12 nm, lateral size of a few microns; Figure 1 A and B; Figure S1A–C). The sizes of GLM are tunable between 5 to 80 μL by predefining the volume of water droplets used (Figure 1 C; Figure S1D), indicating the versatile reaction capacity of such miniature reactors. The shell thickness is estimated to be about 220 μm (see the Supporting Information 1). GLM also exhibit high contact angles of $>150°$ (effective surface tension $\approx 59\ mJ\ m^{-2}$; Figures S1D and S2) and a low slip-off angle of about 20°

[*] W. Gao,[+] H. K. Lee,[+] Prof. X. Y. Ling
Division of Chemistry and Biological Chemistry
School of Physical and Mathematical Sciences
Nanyang Technological University
50 Nanyang Avenue, Singapore 637371 (Singapore)
E-mail: xyling@ntu.edu.sg

W. Gao,[+] Prof. T. Liu
State Key Laboratory of Molecular Engineering of Polymers
Department of Macromolecular Science, Fudan University
Shanghai 200433, (P. R. China)
E-mail: txliu@fudan.edu.cn

H. K. Lee,[+] Dr. I. Y. Phang
Institute of Materials Research and Engineering
A*STAR (Agency for Science, Technology and Research)
3 Research Link, Singapore 117602 (Singapore)
E-mail: phangiy@imre.a-star.edu.sg

Dr. J. Hobley
Department of Chemistry, University of Brunei Darussalam
Jalan Tungku Link, Gadong, BE1410 (Brunei Darussalam)

[+] These authors contributed equally to this work.

[**] X.Y.L. thanks for support from the National Research Foundation, Singapore (NRF-NRFF2012-04), and the Nanyang Technological University's start-up grant. T.L. and W.G. are grateful for support from the National Natural Science Foundation of China (51125011, 51433001). W.G. thanks for support from the China Scholarship Council. H.K.L. thanks for support from A*STAR Graduate Scholarship, Singapore.

Supporting information for this article is available on the WWW under http://dx.doi.org/10.1002/anie.201412103.

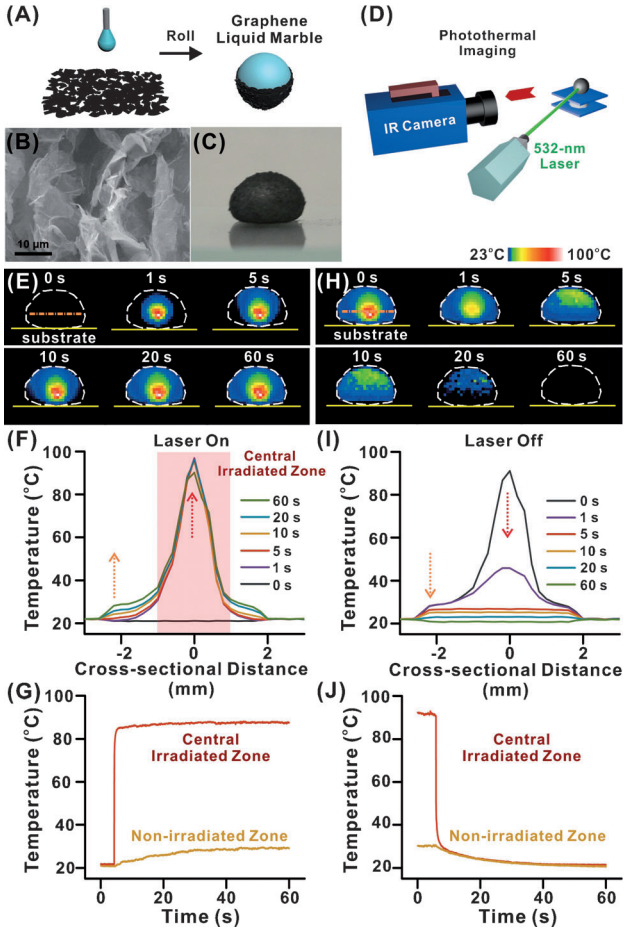

Figure 1. A) Preparation of graphene liquid marble (GLM). B) SEM image of perfluorooctylsilane-grafted graphene nanoplatelets. C) Digital image of a 40 μL GLM. D) Schematic representation of the photothermal set-up. E,H) Thermograms, F,I) spatial temperature profiles, and G,J) temperature-time profiles of GLM when the irradiation laser is switched on and off, respectively. The orange dotted lines denote the locations where (F,I) are obtained. Central irradiated and non-irradiated zone are assigned at cross-sectional distance of 0 mm and $\geq \pm 1$ mm, respectively. Laser power = 112 mW.

(Figure S1E), clearly demonstrating their excellent nonstick properties and ability to isolate encapsulated liquid from the underlying platform.

The photothermal behavior of GLM is investigated upon laser irradiation (532 nm, laser power = 112 mW), and its spatially resolved, front-temperature profiles are monitored using an infrared (IR) camera (Figures 1 D and S3A). Prior to laser irradiation, a 40 μL GLM exhibits a homogeneous surface temperature of 21 °C (Figure 1 E, 0 s). Within 1 s of irradiation, the surface temperature of the central irradiated zone (cross-sectional distance = 0 mm) instantaneously increases to about 90 °C (Figure 1 F), with a temperature change rate $(dT/dt)_{max}$ of ca. 600 °C s^{-1} (Figure S4A). The temperature at the central irradiated zone remains plateau at 90 °C throughout 60 s of laser irradiation (Figure 1 G). The spatial–temperature plots exhibit Gaussian-like profiles, indicating localized photothermal heating due to the use of a Gaussian laser beam (Figure S5).[11]

We also note a slower heat conduction process from the central irradiated zone to the nonirradiated zone (cross-sectional distance $\geq \pm 1$ mm) through the thermally conductive GLM. Such heat transfer results in a gradual temperature increase on the nonirradiated surface from 21 to 30 °C after 60 s of laser irradiation (Figure 1 F,G), during which $(dT/dt)_{max} \approx 0.5$ °C s^{-1} (Figure S4B). The heat conduction on GLM is further evidenced by its lateral-profile photothermal imaging (Figure S6), in which the temperature elevates progressively across the entire graphene shell.

Generally, the photothermal behavior of GLM can be categorized as a two-step heating process. Firstly, the drastic temperature increment is attributed to the instantaneous photothermalization of light (< 10 ps) by graphene.[8] A subsequent temperature plateau indicates that a thermal equilibrium is reached, in which the photothermal heat generation is balanced by heat dissipation through thermal conduction to the entire graphene shell, the encapsulated water, and the environment. In contrast, no temperature change is observed on an irradiated 40 μL water droplet (to be discussed later), affirming that the photothermal responses of our GLM originate from their graphene shells. The photothermal efficiency of GLM (η), which is the ratio of the thermal energy to the total irradiation energy,[12] is estimated to be 15 % (Figure S7) and is comparable to most graphene-based photothermal agents.[9a,b,13]

Next, the cooling process of the GLM is studied by switching off the laser. Similarly, the cooling process at the central irradiation zone occurs in two stages (Figure 1 H,I,J); an initial rapid temperature decrease from about 90 to 46 °C within 1 s ($(dT/dt)_{max} \approx -600$ °C s^{-1}; Figure S4), followed by a gradual temperature decrease of the entire graphene surface to the preheated state of 21 °C within 60 s ($(dT/dt)_{max} \approx -0.5$ °C s^{-1}). The longer duration of the cooling process to achieve thermal equilibrium ($\approx$ 30 s) is possibly due to a slower heat dissipation from the graphene shell to air. Overall, the results highlight the instantaneous photothermal properties of GLM, and also its high thermal conductivity to achieve rapid thermal modulation.[11,14] Hereafter, for the ease of discussion, only the maximum surface temperature (central irradiated zone) of GLM will be discussed.

The surface temperature of our GLM can also be modulated by the irradiation laser power. Equilibrium temperature (at t = 60 s) from 33 to 135 °C are achieved by tuning the laser power from 11 to 214 mW, respectively (Figure 2 A). Similar Gaussian-like spatial temperature profiles and a two-stage heating process are observed (Figure 2 A,B). The thermal energy generated at the graphene shell can subsequently be conducted to heat the encapsulated water (to be discussed later). Upon turning off the laser, GLM rapidly cools to about 21 °C in 60 s (Figure 2 C). Both heating and cooling processes demonstrate linear temperature responses to the applied laser power (Figure 2 D), highlighting the tunable, wide temperature range on GLM at the instance of laser irradiation.

The rapid responsiveness and high reproducibility of photothermal heating are further illustrated by subjecting a 40 μL GLM to heating/cooling cycles on laser irradiation (112 mW). We observe the precise cycling of GLM surface

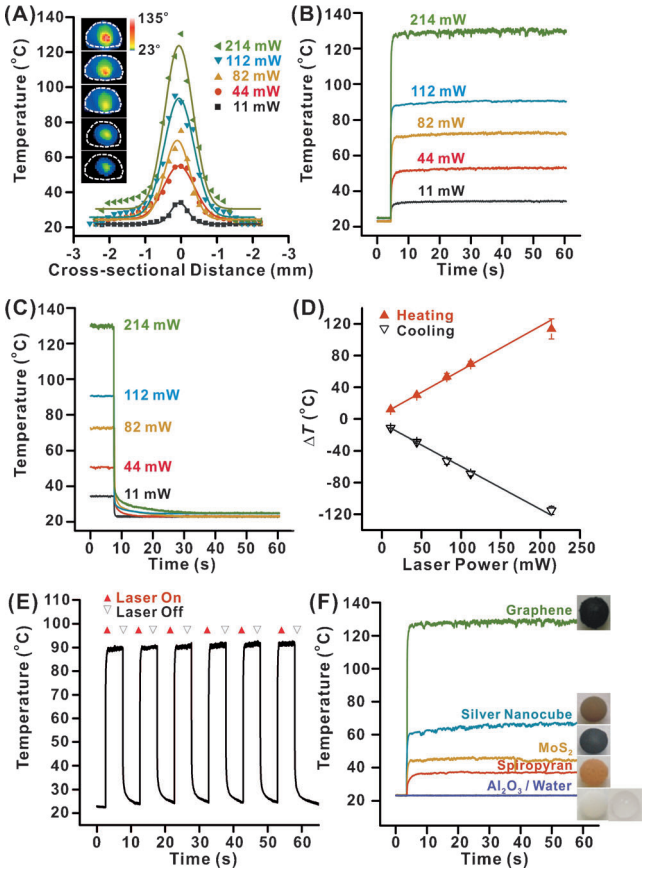

Figure 2. A) Gaussian-fitted spatial temperature profiles of GLM at different laser power ($t = 60$ s). Temperature–time profiles on GLM when the irradiation laser is switched (B) on and (C) off. D) Temperature changes of GLM with laser power. E) Heat/cool cycling test on GLM (laser power = 112 mW). F) Temperature–time profiles of liquid marbles prepared from various encapsulating materials (laser power = 214 mW). (B–F) indicate maximum surface temperature. All volumes are 40 µL.

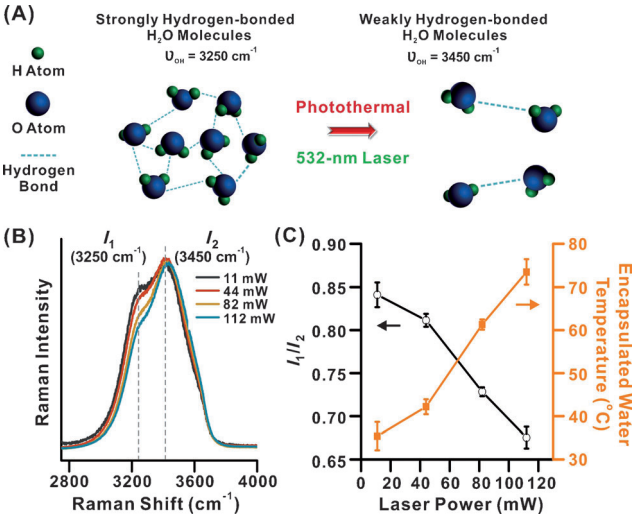

Figure 3. Raman-based determination of the temperature of encapsulated water in GLM. A) Illustration of the differences in interaction between water molecules during photothermal heating. B) Raman spectra and C) I_1/I_2 ratio and corresponding temperature of encapsulated water in GLM, at different irradiation laser powers.

temperature between 21 and 90 °C over six successive cycles (Figure 2E). Such photothermal heating is also highly reproducible across different volumes of GLM (Figure S9). Hence, GLM clearly enables timely and precise thermal control essential for temperature-sensitive reactions.

GLM possesses more superior photothermal heating over liquid marbles formed using other materials. Upon laser irradiation (214 mW), GLM exhibits the highest surface temperature of about 135 °C (Figure 2F), which is ≥2-fold higher than liquid marbles of other materials (≤65 °C). We affirm the temperature rise originates from photothermal heating on the encapsulating materials, as evident from the negligible temperature response from water ($T = 23$ °C). The lower temperature increment of these controls is possibly due to weaker photoabsorption and photothermal efficiency at 532 nm.

Thus far, only the surface temperature of GLM is examined and the determination of actual encapsulated water temperature is also crucial for a latter application as remotely heatable miniature reactor. Here, the encapsulated water temperature of 40 µL GLM is quantified using the Raman fingerprint of water (Figure 3A). All spectra exhibit water bimodal OH stretchings, with characteristic temperature-dependent Raman bands at 3250 cm^{-1} (I_1) and 3450 cm^{-1} (I_2) (Figure 3B), assigned to strongly and weakly hydrogen-bonded water molecules,[15] respectively. Generally, elevated temperature disrupts the hydrogen bonding between water molecules and reduces the proportion of strongly hydrogen-bonded water molecules. Our observation agrees well with the literature; the ratio of I_1/I_2 decreases from 0.84 to 0.68 as laser power increases from 11 to 112 mW (Figure 3C), respectively. Hence, the temperature of water encapsulated in GLM is determined to range between 35 to 74 °C (Figure S10). In contrast, the non-photothermal Al_2O_3-liquid marble control exhibits a constant I_1/I_2 ratio with varying laser power (Figure S10). Hence, the photothermal heat generated on the thermally conductive graphene shell can clearly modulate the temperature of encapsulated water.

GLM as a remotely heatable miniature reactor is evaluated by studying the temperature-dependent degradation of methylene blue (Figure 4A). Typically, 40 µL GLM, containing 1 mM methylene blue and 0.4 M $NaBH_4$, are irradiated using a laser power of 112 mW. At predefined time intervals, we extracted the encapsulated aqueous solution and observed a steady decrease of the characteristic 665 nm extinction peak intensity of methylene blue (Figure 4B),[6] indicating its degradation over laser irradiation time. Consequently, a degradation efficiency of >70% is achieved ($C/C_0 = 0.3$; C_0 and C denote the initial concentration and concentration at time t, respectively) after 10 min of photothermal heating (Figures S11 and S12). In contrast, only ≤10% of the degradation efficiency is achieved in the absence of photothermal heating or $NaBH_4$, probably due to contributions from photobleaching, heat-induced molecular transformation, and/or adsorption of methylene blue (Figures 4C, S12, and S13). The methylene blue reduction by $NaBH_4$ is assumed to be

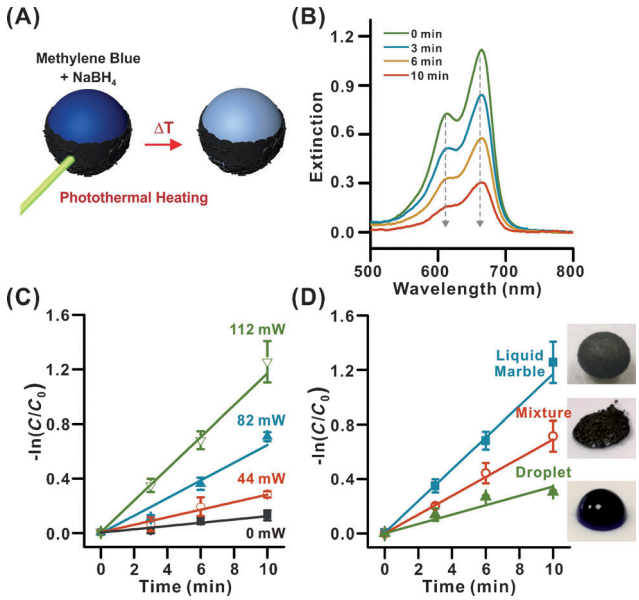

Figure 4. A) Schematic representation of GLM as remotely heatable miniature reactor. B) Extinction spectra of methylene blue solution extracted from GLM at different time intervals (laser power = 112 mW). Plot of $-\ln(C/C_0)$ against irradiation duration for C) different laser power applied and D) different types of miniature reactor. All volumes are 40 μL.

a pseudo-first-order reaction; $\ln(C/C_0) = -k_{app}t$, in which k_{app} and t denote the degradation rate constant and time, respectively.[6] Consequently, k_{app} is calculated at 0.01 and 0.12 min^{-1} for a laser power of 0 and 112 mW (Figure 4C), respectively. Hence, remotely heatable GLM provide tremendous enhancement in both the degradation efficiency (> 7-fold), and reaction kinetics (> 12-fold) of the methylene blue degradation reaction compared to the absence of photothermal heating.

The temperature-dependent reaction kinetics of methylene blue degradation can also be modulated by the laser power. By tuning the laser power to 44 and 82 mW, k_{app} is easily modulated to 0.03 and 0.06 min^{-1} (Figure 4C), respectively. Excluding potential effects from encapsulated water evaporation (Figure S14), the dependency of reaction kinetics on the temperature clearly follows the Arrhenius equation (Figure S15).[10] Such a thermal modulation of reaction kinetics by localized heating therefore makes GLM the first demonstration of a remotely heatable and isolated miniature reactor, with > 5-fold prolonged lifetime compared to conventional bulk heating (Figure S14). The importance of GLM is again highlighted in comparison with bare reaction solution droplets and graphene solution mixtures (Figure 4D); only GLM provides an isolated environment and exhibits ≥ 1.7-fold superior degradation rate constant (Figure S16).

In summary, graphene liquid marbles have been fabricated as robust, isolated, and remotely heatable miniature reactors for the enhancement of methylene blue reaction kinetics by more than twelve times, achieving > 70% degradation efficiency. GLM also demonstrates rapid, reproducible, and strong photothermal heating to achieve encapsulated water temperatures ranging between 21 to 74 °C, simply by varying the laser power. The ensemble of benefits enables GLM as an attractive miniature reactor for a vast library of reactions, including heat-activated processes and reaction kinetics modulation. This is crucial in fields involving costly and hazardous conditions, in which small-scale preliminary reactions are preferred. The inhibition of encapsulated water evaporation and studies of thermal flow within GLM are currently under investigation.

Keywords: graphene · liquid marble · miniature reactors · photothermal reactions · reaction kinetics modulation

How to cite: *Angew. Chem. Int. Ed.* **2015**, *54*, 3993–3996
Angew. Chem. **2015**, *127*, 4065–4068

[1] a) P. Aussillous, D. Quere, *Nature* **2001**, *411*, 924–927; b) E. Bormashenko, *Soft Matter* **2012**, *8*, 11018–11021; c) E. Bormashenko, *Curr. Opin. Colloid Interface Sci.* **2011**, *16*, 266–271; d) E. Bormashenko, Y. Bormashenko, R. Pogreb, O. Gendelman, *Langmuir* **2011**, *27*, 7–10.
[2] a) H. K. Lee, Y. H. Lee, I. Y. Phang, J. Wei, Y.-E. Miao, T. Liu, X. Y. Ling, *Angew. Chem. Int. Ed.* **2014**, *53*, 5054–5058; *Angew. Chem.* **2014**, *126*, 5154–5158; b) G. McHale, M. I. Newton, *Soft Matter* **2011**, *7*, 5473–5481.
[3] T. Arbatan, L. Li, J. Tian, W. Shen, *Adv. Healthcare Mater.* **2012**, *1*, 80–83.
[4] Y. Chu, Z. Wang, Q. Pan, *ACS Appl. Mater. Interfaces* **2014**, *6*, 8378–8386.
[5] Y. Xue, H. Wang, Y. Zhao, L. Dai, L. Feng, X. Wang, T. Lin, *Adv. Mater.* **2010**, *22*, 4814–4818.
[6] Y.-E. Miao, H. K. Lee, W. S. Chew, I. Y. Phang, T. Liu, X. Y. Ling, *Chem. Commun.* **2014**, *50*, 5923–5926.
[7] F. Bonaccorso, Z. Sun, T. Hasan, A. C. Ferrari, *Nat. Photonics* **2010**, *4*, 611–622.
[8] G. D. Sanders, C. J. Stanton, J. H. Kim, K. J. Yee, M. H. Jung, B. H. Hong, L. G. Booshehri, E. H. Hàroz, J. Kono, *AIP Conf. Proc.* **2011**, *1416*, 31–33.
[9] a) D. Meng, S. Yang, L. Guo, G. Li, J. Ge, Y. Huang, C. W. Bielawski, J. Geng, *Chem. Commun.* **2014**, *50*, 14345–14348; b) C.-a. Tao, X. Zou, Z. Hu, H. Liu, J. Wang, *Polym. Compos.* **2014**, DOI: 10.1002/pc.23303; c) Y. Xue, Y. Liu, F. Lu, J. Qu, H. Chen, L. Dai, *J. Phys. Chem. Lett.* **2012**, *3*, 1607–1612.
[10] J. Qiu, W. D. Wei, *J. Phys. Chem. C* **2014**, *118*, 20735–20749.
[11] T. Hong, Y. Cao, D. Ying, Y.-Q. Xu, *Appl. Phys. Lett.* **2014**, *104*, 223102-1–223102-5.
[12] H. Chen, L. Shao, T. Ming, Z. Sun, C. Zhao, B. Yang, J. Wang, *Small* **2010**, *6*, 2272–2280.
[13] V. Abdelsayed, S. Moussa, H. M. Hassan, H. S. Aluri, M. M. Collinson, M. S. El-Shall, *J. Phys. Chem. Lett.* **2010**, *1*, 2804–2809.
[14] J. H. Seol, I. Jo, A. L. Moore, L. Lindsay, Z. H. Aitken, M. T. Pettes, X. Li, Z. Yao, R. Huang, D. Broido, N. Mingo, R. S. Ruoff, L. Shi, *Science* **2010**, *328*, 213–216.
[15] J. Hobley, Y. Kuge, S. Gorelik, M. Kasuya, K. Hatanaka, S. Kajimoto, H. Fukumura, *Phys. Chem. Chem. Phys.* **2008**, *10*, 5256–5263.

Received: December 17, 2014
Revised: January 8, 2015
Published online: February 4, 2015

